Editors' Suggestion

Measurement of Penrose Superradiance in a Photon Superfluid

Maria Chiara Braidotti,[1,*] Radivoje Prizia,[1,2] Calum Maitland,[2] Francesco Marino,[3,4] Angus Prain,[1] Ilya Starshynov,[1] Niclas Westerberg,[1] Ewan M. Wright,[5] and Daniele Faccio[1,5,†]

[1]School of Physics and Astronomy, University of Glasgow, G12 8QQ Glasgow, United Kingdom
[2]Institute of Photonics and Quantum Sciences, Heriot-Watt University, EH14 4AS Edinburgh, United Kingdom
[3]CNR-Istituto Nazionale di Ottica, Largo Enrico Fermi 6, I-50125 Firenze, Italy
[4]INFN, Sezione di Firenze, Via Sansone 1, I-50019 Sesto Fiorentino (FI), Italy
[5]Wyant College of Optical Sciences, University of Arizona, Tucson, Arizona 85721, USA

(Received 4 August 2021; accepted 30 November 2021; published 4 January 2022)

The superradiant amplification in the scattering from a rotating medium was first elucidated by Sir Roger Penrose over 50 years ago as a means by which particles could gain energy from rotating black holes. Despite this fundamental process being ubiquitous also in wave physics, it has only been observed once experimentally, in a water tank. Here, we measure this amplification for a nonlinear optics experiment in the superfluid regime. In particular, by focusing a weak optical beam carrying orbital angular momentum onto the core of a strong pump vortex beam, negative norm modes are generated and trapped inside the vortex core, allowing for amplification of a reflected beam. Our experiment demonstrates amplified reflection due to a novel form of nonlinear optical four-wave mixing, whose phase-relation coincides with the Zel'dovich-Misner condition for Penrose superradiance in our photon superfluid, and unveil the role played by negative frequency modes in the process.

DOI: 10.1103/PhysRevLett.128.013901

Introduction.—Penrose superradiance is the process by which energy can be extracted from a rotating black hole via a scattering process in which an object splits in two at the ergosphere, with one part falling into the ergoregion where it will have negative energy and therefore providing a positive energy gain to the reflected or scattered part of the object [1]. The role of negative frequencies in rotational amplification of waves was subsequently investigated in a different setting by Zel'dovich, who showed that electromagnetic waves incident radially on a rotating metallic cylinder could be amplified if the cylinder spins fast enough to allow negative Doppler-shifted wave frequencies [2], with several proposals for experiments in various settings [3–7] and an experimental demonstration using acoustic waves [8].

Astrophysical Penrose superradiance has to date not been observed with current technology, in part, due to the large distances between Earth and the nearest rotating black hole. However, proposals based on analog gravity have led to the first experimental observation of superradiance, reported in a hydrodynamic experiment [9], also related to so-called overreflection [10–14].

In this arena, photon superfluids have proved to be a versatile platform [15–26], and recently the concept of rotational Penrose amplification has been extended to the superfluid regime, where Bogoliubov excitations act as particles in the Penrose picture [27–31]. Moreover, we have recently shown that superradiance arises naturally in nonlinear optics in the superfluid regime [29,31]. Briefly, it was shown that a wave incident at glancing angle onto the ergoregion of a rotating photon fluid undergoes a splitting into positive and negative frequency components. The Zel'dovich-Misner condition for superradiance $\omega - m\Omega < 0$ (ω is the oscillation frequency of a wave that has orbital angular momentum m, and Ω is the system rotation frequency) now takes the form of a phase-matching relation, which if met allows for the negative frequency modes to be trapped and amplification of the positive frequency modes to occur.

In this Letter, we report measurements of Penrose rotational superradiance in nonlinear optics. Thanks to the recent findings reported in Refs. [29,31], we experimentally test the nonlinear interaction of a weakly focused probe beam having orbital angular momentum (OAM) and corotating with a strong copropagating vortex pump beam. We demonstrate that amplification occurs only if the superradiance condition is met, and idler waves, which play the role of negative energy modes, are generated and trapped inside the pump ergoregion. The presence of a negative current near the pump vortex core is a key component that underpins the physical amplification process of Penrose superradiance and had not been observed before. Photon fluids therefore allow for the study of the fundamental inner workings of Penrose superradiance, including, e.g., the details and influence of negative-mode trapping and transient phenomena that are not accessible in other systems.

The model.—We consider the nonlinear interaction between a pump beam E_0 and a weak signal beam E_s,

with orbital angular momenta ℓ and n, respectively. The two fields are monochromatic with the same wavelength λ, and are copropagating along the z axis in a thermo-optic nonlinear medium [23,24]. The geometry of the process is depicted in Fig. 1. Specifically, the collimated pump vortex E_0 is shown as the gray beam in Fig. 1, and the signal beam E_s (green beam in Fig. 1) is loosely focused onto the vortex core. The total optical field can then be written as $E = E_0 + E_s + E_i$, where E_i is the "idler" beam (red beam in Fig. 1) generated by the nonlinear interaction of the pump E_0 with the signal field E_s, and whose OAM is $q = (2\ell - n)$. The evolution of the total field E is governed in the paraxial regime by the nonlinear Schrödinger equation (NSE) [32]

$$i\frac{\partial E}{\partial z} + \frac{1}{2k}\nabla_\perp^2 E + \frac{k}{n_0}\Delta n(|E|^2)E = 0, \tag{1}$$

where n_0 is the linear refractive index, $k = 2\pi n_0/\lambda = n_0 k_0$ is the wave number, and $\nabla_\perp^2$ is the transverse Laplacian describing beam diffraction. Equation (1) is akin to the Gross-Pitaevskii equation for a two-dimensional (2D) superfluid, with $E(x, y, z)$ being the order parameter and z playing the role of time. For this photon superfluid, the photon-photon repulsive interaction is mediated through the heating induced by the local intensity of the propagating beam. The specific thermo-optic medium used for the experiment is composed of a solution of methanol and a low concentration

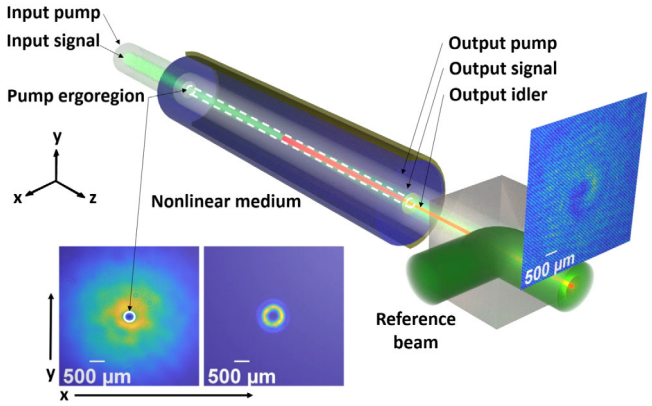

FIG. 1. Illustration of the experimental interaction geometry. The pump (gray) beam propagates inside the nonlinear sample copropagating along the z axis with the signal (green) beam. The dashed white line represents the ergoregion encircling the pump core. The signal beam is loosely focused onto the pump core and after the focus, if superradiance occurs, an idler (red) beam is generated and is trapped inside the ergoregion. A reference beam interferes with the total field at the output of the sample. The inset shows experimental image examples of the pump (left, $\ell = 1$) and signal (right, $n = 2$) beam transverse profiles at the input. The white line in the pump inset shows the ergoregion location ($r_e = 118\ \mu$m). The experimental parameters for the beams shown are pump Gaussian waist $w_0^{bg} \simeq 1$ cm, core waist $w_0^v \simeq 100\,\mu$m, and the signal core waist $w_s^v \simeq 150\ \mu$m.

of graphene nanoflakes (23×10^{-6} g/cm^3), providing a weak absorption of the pump input beam to enhance the thermo-optic nonlinearity [33]. In this system, the nonlinear refractive index perturbation Δn in steady state is [24]

$$\Delta n(\mathbf{r}) = n_2 \int R(\mathbf{r} - \mathbf{r}')|E(\mathbf{r}')|^2 d\mathbf{r}', \tag{2}$$

where $\mathbf{r} = (x, y)$ and $n_2 < 0$ is the nonlinear coefficient for the defocusing nonlinearity. For thermo-optic nonlinearities, the nonlocal response function R can be written as $R(\mathbf{r}) = [1/(2\pi\sigma^2)]K_0(|\mathbf{r}|/\sigma)$, where $K_0(s)$ is the zeroth-order modified Bessel function of the second kind, with σ being the transverse scale of the nonlocality [24,35]. Moreover, experiments with time gated measurements [24], performed over short times (~0.2 s in our case), have verified that a strong nonlinearity with a weak nonlocality ($\sigma \sim 200\ \mu$m) can be realized before thermal diffusion has reached the steady state (around 20 s in our case).

Our experiment employs short data acquisition times and we hereafter treat the photon fluid system as quasilocal [24] and adopt the local theory reported in Ref. [31].

To proceed, we describe the physics of the Penrose superradiance in a photon fluid, a more mathematical treatment being available in Ref. [31] and also the Supplemental Material [34]. In photon fluids, perturbations composed of the signal and idler beams can form oscillations in the transverse (x, y) plane that behave as phononic modes [31]. Superradiance then emerges from judicious choice of the interaction geometry that allows for balancing of the incoming signal that focuses onto and then glances off the pump core along with concomitant generation of an idler beam that can, under appropriate waveguiding conditions, remain trapped inside the pump vortex core (where the refractive index is higher than the surrounding high-intensity region). This interaction geometry leads to a geometry-induced phase-matching condition that allows for energy transfer from the pump beam into the signal and the idler modes. More specifically, while the signal focus glances off the pump core, it undergoes a phase shift due to the combination of the nonlinearity and the focusing (Gouy phase shift in optics). The amplification of the signal is then intimately connected to the excitation of the guided idler mode inside the core of the pump beam core [31]. Mathematically, superradiance occurs if $\Delta K = \Delta K_s + \Delta K_i > 0$ (phase-matching condition), where $\Delta K_{s,i} = k_{s,i} - \beta_\ell$ are the signal and idler phononic (longitudinal) wave vectors, reduced by the presence of the nonlinear pump. This phase-matching condition expressed in frequencies $\Delta\omega \propto -\Delta K < 0$ ($\Delta\omega = \Delta\omega_s + \Delta\omega_i$) has been shown [31] to map identically onto the Zel'dovich-Misner condition required to observe Penrose superradiance. Intuitively, if we had plane waves, the signal and idler wave vector shifts are $\Delta K_{s,i} < 0$ and their frequencies will both be positive $\Delta\omega_{s,i} > 0$. However, the waveguide

potential adds a positive term to the idler wave vector, which can lead to $\Delta K_i > 0$ and therefore $\Delta\omega_i < 0$.

In the superfluid picture, there are then three conditions to be met in order to observe Penrose superradiance. First, the phase-matching (Zel'dovich-Misner) condition $\Delta\omega \propto -\Delta K < 0$ should be satisfied. Second, the guided idler modes should have negative frequency shifts $\Delta\omega_i < 0$ to conform with the fact that they are trapped within the ergosphere. In the experiments, we explicitly verify the conditions for $\Delta K > 0$ and $\Delta K_i > 0$ (i.e., $\Delta\omega_i < 0$) by numerically evaluating the signal and idler wave vectors, including the contribution from the pump vortex that is modeled as a static waveguide for the idler (see Supplemental Material [34]). Third, the Zel'dovich-Misner condition requires $m = (n - \ell) > 0$ for amplification, i.e., the signal OAM n must be larger than the pump OAM ℓ [31]. This requirement is experimentally determined by the choice of input pump and signal OAM values (see [34]).

Finally, once the experimental conditions are verified, we monitor the presence of superradiance by extracting the phonon currents. We define the reflection and transmission coefficients for scattering from the pump ergoregion r_e (radius at which at which the velocity of the flow equals the speed of the photon fluid [23,34]) using the Noether current J^0. The charge $N(z)$, proportional to the total energy density of the Bogoliubov modes, is a conserved quantity in this system $N(z) = \int_0^\infty J^0(r,z)rdr = \int_0^\infty (|E_S|^2 - |E_I|^2)rdr =$ const, where $\partial_z J^0 = 0$ [29,36]. The reflection and transmission coefficients are [29]

$$R_N(z) = \frac{1}{N(z)} \int_{r_e}^{\infty} (|E_S|^2 - |E_I|^2) rdr, \tag{3}$$

$$T_N(z) = \frac{1}{N(z)} \int_{0}^{r_e} (|E_S|^2 - |E_I|^2) rdr. \tag{4}$$

Since $R_N(z) + T_N(z) = 1$, a transmission $T_N < 0$ implies that we must have an amplified reflection $R_N > 1$. Therefore, the generation of the trapped negative frequency (idler) mode physically underpins the superradiance process and the current $J^0(r)$ evaluated at the output can be used as a tool to prove the presence of Penrose amplification, identified as a negative current $J^0(r) < 0$ inside the ergoregion (trapped idler) and $J^0(r) > 0$ outside $(R_N > 1)$ (reflected signal).

We note that the current formalism also works in the transient regime, where the signal field is still in proximity of the ergoregion and has not reached an ideal observer at infinity [29].

Experiment.—An outline of the experimental setup is shown in Fig. 1 (see Supplemental Material [34] for more details). A continuous-wave Gaussian laser beam of wavelength $\lambda = 532$ nm is split into three beams: the pump beam, the signal beam, and a reference beam. By using two phase masks, we generate the azimuthal phase profiles $\phi = p\theta$, with $p = \ell, n$ the OAM values for the pump and signal beams, respectively (see Supplemental Material [34]). The inset in Fig. 1 shows the transverse intensity profiles of the pump (left) and signal (right) input beams and the corresponding beam waists are given in the caption. The two beams are then incident coaxially onto a cell of radius 1 cm and length 13 cm, filled with a methanol-graphene solution.

An additional lens is used to focus the signal beam into the pump core halfway along the medium. The near-field intensity at the output facet of the medium and the reference plane wave are overlapped at a small angle and imaged onto a CMOS camera. The resulting interferogram allows for the extraction of the pump + signal + idler amplitudes and phases with an off-axis digital holographic reconstruction [37].

The full complex field distribution is then numerically decomposed into Laguerre-Gauss (LG) modes so as to reconstruct the full OAM spectrum and therefore determine the precise relative compositions of the pump and signal and idler fields. In our experiment, we considered two sets of measurements, with pump OAM $\ell = 1$ and 2 (beams core widths of 200 and 300 μm, respectively). The values of the powers (252 and 175 mW, respectively) are chosen in order to have a quasisolitonic evolution of the pump vortex core.

Figure 2 shows the experimentally determined currents $J^0(r)$ versus radius r at the output for various pump and signal OAM combinations and powers: The blue curves for low pump power ($P_p \simeq 10$ mW, so as to negligibly excite any nonlinear effects) have $J^0(r) > 0$ for all radii and superradiance is absent. For the case of pump OAM $\ell = 1$ and high pump power ($P_p \simeq 250$ mW for OAM $\ell = 1$ and $P_p \simeq 175$ mW for OAM $\ell = 2$), shown in Figs. 2(a)–2(d), we analyzed four signal OAMs: $n = 3$, 2 in Figs. 2(a) and 2(b) that satisfy the three conditions for superradiance ($\omega - m\Omega < 0$, $\Delta\omega_i < 0$, $n - \ell > 0$); $n = -1, -2$ in Figs. 2(c) and 2(d) that do not satisfy the three conditions (see Supplemental Material [34]). In particular, for Figs. 2(a) and 2(b), we see that the current $J^0(r)$ is negative within the ergoregion (indicated in all figures by a dashed red line) and positive outside, consistent with the presence of superradiance, whereas $J^0(r) > 0$ for all radii when the superradiance condition is not satisfied, Figs. 2(c) and 2(d).

Figures 2(e)–2(h) report results for a pump OAM $\ell = 2$. The two signal OAMs $n = 4$, 3 in Figs. 2(e) and 2(f) display superradiance with a negative current inside the ergoregion. Figures 2(g) and 2(h) are for signal OAM $n = 1, -1$, which do not satisfy the Zel'dovich-Misner condition and show $J^0(r) > 0$ for all r. The insets in Fig. 2 report the corresponding signal and idler transverse intensity profiles in the vicinity of the pump core, reconstructed from the experimental data using the LG decomposition. In particular, we observe that the signal and idler beams can become spatially separated and that when superradiance

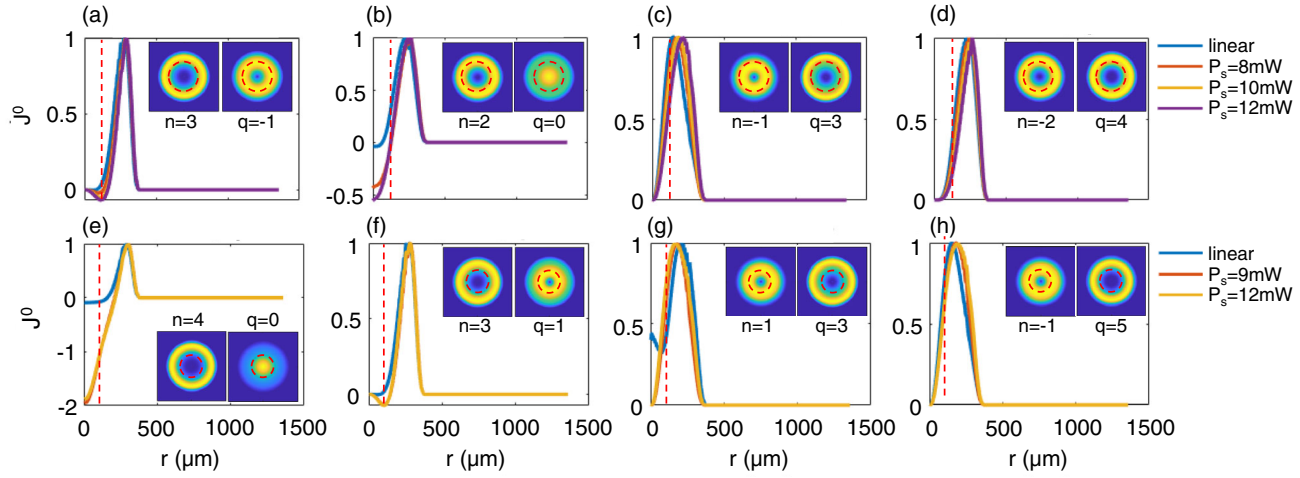

FIG. 2. Experimentally measured currents $J^0(r)$ versus radius r. (a)–(d) Pump OAM $\ell = 1$ and (e)–(h) pump OAM $\ell = 2$. Penrose superradiance conditions are satisfied in (a),(b),(e),(f). (a) Signal has OAM $n = 3$ and idler OAM $q = -1$. (b) $n = 2$ and $q = 0$. (c) $n = -1$ and $q = 3$. (d) $n = -2$ and $q = 4$. (e) $n = 4$ and idler with OAM $q = 0$. (f) $n = 3$, $q = 1$. (g) $n = 1$, $q = 3$. (h) $n = -1$ and $q = 5$. The dashed red lines in all panels indicate the location of the radius r_e of the ergoregion [$r_e = 118$ μm in (a)–(d) and $r_e = 104$ μm in (e)–(h)]. Insets show the output intensity profiles $|E_{s,i}(r)|^2$ reconstructed from measurements verifying that idler trapping in the pump vortex core occurs for the superradiant cases (a),(b),(e),(f).

occurs the idler beam is trapped inside the ergoregion. This is most apparent in the examples with idler $q = 0$ in Figs. 2(b) and 2(e) where the trapped idler mode has zero OAM and is peaked in the center of the pump vortex.

These results therefore experimentally validate within a wide range of conditions the predicted connection between the Zel'dovich-Misner condition for Penrose superradiance and the excitation of negative norm idler modes.

Figure 3 shows the reflection coefficient R_N calculated at the medium output for all the pump and signal OAM combinations and different signal input powers. The reflection R_N from the ergoregion is calculated using Eq. (3) as a function of $m = n - \ell$ (lower axes). The data points for which $m = n - \ell > 0$ is verified together with the other two superradiance conditions outlined above, i.e., $\omega - m\Omega < 0$ and $\Delta\omega_i < 0$ are circled with a dashed line (see Supplemental Material [34]). As can be seen, only these points show evidence of overreflection, $R_N > 1$, and all other points have $R_N \leq 1$. A maximum amplification of 5% is observed when the idler OAM is $q = 0$ (upper axes), consistent with the fact that the trapped idler is strongly localized in the pump vortex core. The trend of R_N with $m = n - \ell$ is also confirmed by numerical simulations (see Supplemental Material [34]).

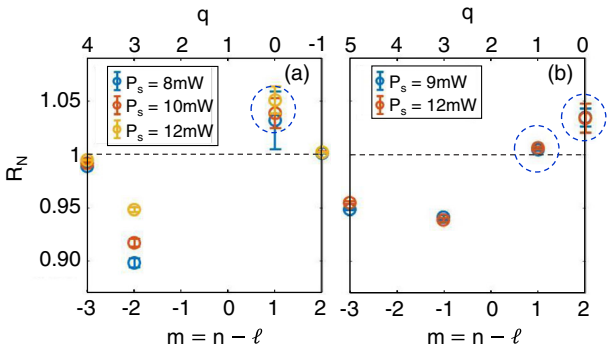

FIG. 3. Reflection coefficient R_N, calculated at the sample output ($z = 13$ cm), as a function of signal and pump OAM difference $m = n - \ell$ (lower axes) and idler OAM q (upper axes) for (a) pump $\ell = 1$ and (b) pump $\ell = 2$. Amplification with $R_N > 1$ is observed for $m = n - \ell > 0$. All values of R_N are calculated from the average over 20 different acquisitions and the standard deviation is used to determine the error bars. Blue dashed circles indicate the configurations where superradiance conditions ($\Delta K > 0$, $\Delta K_i > 0$, and $m = n - \ell > 0$) are satisfied (see Supplemental Material [34]).

Conclusions.—Penrose superradiance was originally predicted as an astrophysical process in which positive energy modes are amplified from the interaction with a rotating black hole, at the expense of their negative energy counterpart, which remains trapped inside the rotating body. This concept was first tested in hydrodynamics with water waves scattering from a vortex in a bath tub. The results presented in this Letter show the arising of a novel process of wave mixing in nonlinear optics inspired by Penrose superradiance physics. We measure amplification of positive energy modes with OAM in the scattering with a rotating background. The trapping of the negative energy counterpart is also measured thanks to the Noether current formalism. We measure an overreflection (reflectivity greater than 1) revealing the presence of superradiance even in the transient regime. This experiment provides a novel and accessible platform for investigating Penrose superradiance, deepening our understanding of the physics at a fundamental level and, for example, providing a

platform for future studies investigating energy extraction from superfluid vortices.

Open access data is available at Ref. [38].

The authors acknowledge financial support from EPSRC (UK Grant No. EP/P006078/2) and the European Union's Horizon 2020 research and innovation program, Grant Agreement No. 820392. N. W. wishes to acknowledge support from the Royal Commission for the Exhibition of 1851. The authors would like to thank Bienvenu Ndagano for the fruitful discussions and valuable suggestions throughout this project.

*Corresponding author.
mariachiara.braidotti@glasgow.ac.uk
†Corresponding author.
daniele.faccio@glasgow.ac.uk

[1] R. Penrose, Gravitational collapse: The role of general relativity, Riv. Nuovo Cimento **1**, 252 (1969) [Gen. Relativ. Gravit. **34**, 1141 (2002)].
[2] Y. B. Zel'dovich, Generation of waves by a rotating body, Pis'ma Zh. Eksp. Teor. Fiz. **14**, 270 (1971) [JETP Lett. **14**, 180 (1971)].
[3] C. Gooding, S. Weinfurtner, and W. G. Unruh, Reinventing the Zel'dovich wheel, Phys. Rev. A **101**, 063819 (2020).
[4] M. C. Braidotti, A. Vinante, G. Gasbarri, D. Faccio, and H. Ulbricht, Zel'dovich Amplification in a Superconducting Circuit, Phys. Rev. Lett. **125**, 140801 (2020).
[5] C. Gooding, S. Weinfurtner, and W. G. Unruh, Superradiant scattering of orbital angular momentum beams, Phys. Rev. Research **3**, 023242 (2021).
[6] D. Faccio and E. M. Wright, Superradiant Amplification of Acoustic Beams via Medium Rotation, Phys. Rev. Lett. **123**, 044301 (2019).
[7] C. Gooding, Dynamics landscape for acoustic superradiance, Phil. Trans. R. Soc. A **378**, 20200003 (2020).
[8] M. Cromb, G. Gibson, E. Toninelli, M. Padgett, E. M. Wright, and D. Faccio, Amplification of waves from a rotating body, Nat. Phys. **16**, 1069 (2020).
[9] T. Torres, S. Patrick, A. Coutant, M. Richartz, E. W. Tedford, and S. Weinfurtner, Rotational superradiant scattering in a vortex flow, Nat. Phys. **13**, 833 (2017).
[10] A. Fridman, E. Snezhkin, G. Chernikov, A. Rylov, K. Titishov, and Y. Torgashin, Over-reflection of waves and over-reflection instability of flows revealed in experiments with rotating shallow water, Phys. Lett. A **372**, 4822 (2008).
[11] H. S. Ribner, Reflection, transmission, and amplification of sound by a moving medium, J. Acoust. Soc. Am. **29**, 435 (1957).
[12] J. W. Miles, On the reflection of sound at an interface of relative motion, J. Acoust. Soc. Am. **29**, 226 (1957).
[13] D. J. Acheson, On over-reflexion of sound at an interface of relative motion, J. Fluid Mech. **77**, 433 (1976).
[14] S.-I. Takehiro and Y.-Y. Hayashi, Over-reflection and shear instability in a shallow-water model, J. Fluid Mech. **236**, 259 (1992).
[15] Y. Pomeau and S. Rica, Diffraction non linéaire, C. R. Acad. Sci. Paris **317**, 1287 (1993).
[16] R. Y. Chiao and J. Boyce, Bogoliubov dispersion relation and the possibility of superfluidity for weakly interacting photons in a two-dimensional photon fluid, Phys. Rev. A **60**, 4114 (1999).
[17] W. Wan, S. Jia, and J. Fleischer, Dispersive, superfluid-like shock waves in nonlinear optics, Nat. Phys. **3**, 46 (2007).
[18] N. Ghofraniha, C. Conti, G. Ruocco, and S. Trillo, Shocks in Nonlocal Media, Phys. Rev. Lett. **99**, 043903 (2007).
[19] D. Gerace and I. Carusotto, Analog Hawking radiation from an acoustic black hole in a flowing polariton superfluid, Phys. Rev. B **86**, 144505 (2012).
[20] M. Elazar, V. Fleurov, and S. Bar-Ad, All-optical event horizon in an optical analog of a Laval nozzle, Phys. Rev. A **86**, 063821 (2012).
[21] I. Carusotto, Superfluid light in bulk nonlinear media, Proc. R. Soc. A **470**, 20140320 (2014).
[22] P.-E. Larré and I. Carusotto, Propagation of a quantum fluid of light in a cavityless nonlinear optical medium: General theory and response to quantum quenches, Phys. Rev. A **92**, 043802 (2015).
[23] D. Vocke, T. Roger, F. Marino, E. M. Wright, I. Carusotto, M. Clerici, and D. Faccio, Experimental characterization of nonlocal photon fluids, Optica **2**, 484 (2015).
[24] D. Vocke, K. Wilson, F. Marino, I. Carusotto, E. M. Wright, T. Roger, B. P. Anderson, P. Ohberg, and D. Faccio, Role of geometry in the superfluid flow of nonlocal photon fluids, Phys. Rev. A **94**, 013849 (2016).
[25] Q. Fontaine, T. Bienaimé, S. Pigeon, E. Giacobino, A. Bramati, and Q. Glorieux, Observation of the Bogoliubov Dispersion in a Fluid of Light, Phys. Rev. Lett. **121**, 183604 (2018).
[26] D. Vocke, C. Maitland, A. Prain, F. Biancalana, F. Marino, E. M. Wright, and D. Faccio, Rotating black hole geometries in a two-dimensional photon superfluid, Optica **5**, 1099 (2018).
[27] F. Marino, Acoustic black holes in a two-dimensional "photon fluid," Phys. Rev. A **78**, 063804 (2008).
[28] F. Marino, M. Ciszak, and A. Ortolan, Acoustic superradiance from optical vortices in self-defocusing cavities, Phys. Rev. A **80**, 065802 (2009).
[29] A. Prain, C. Maitland, D. Faccio, and F. Marino, Superradiant scattering in fluids of light, Phys. Rev. D **100**, 024037 (2019).
[30] D. D. Solnyshkov, C. Leblanc, S. V. Koniakhin, O. Bleu, and G. Malpuech, Quantum analogue of a Kerr black hole and the Penrose effect in a Bose-Einstein condensate, Phys. Rev. B **99**, 214511 (2019).
[31] M. C. Braidotti, D. Faccio, and E. M. Wright, Penrose Superradiance in Nonlinear Optics, Phys. Rev. Lett. **125**, 193902 (2020).
[32] R. W. Boyd, *Nonlinear Optics*, 2nd ed. (Academic Press, New York, 2002).
[33] This absorption is not displayed in Eq. (1) for simplicity in the presentation; it will be included in the simulations provided in the Supplemental Material [34]. We verified that, despite the presence of losses in NSE photon fluids, the physics of the process is persistent.
[34] See Supplemental Material at http://link.aps.org/supplemental/10.1103/PhysRevLett.128.013901 for further

details on the experimental setup, data analysis and numerical simulations.

[35] T. Roger, C. Maitland, K. Wilson, N. Westerberg, D. Vocke, E. M. Wright, and D. Faccio, Optical analogues of the Newton-Schrodinger equation and boson star evolution, Nat. Commun. **7**, 13492 (2016).

[36] A small optical absorption is present in our system as outlined before. Through numerical simulations, provided in the Supplemental Material [34], we verified that the physics of the process persists and the definition of the reflectivity and transmission holds also in the case of small losses.

[37] E. Cuche, P. Marquet, and C. Depeursinge, Spatial filtering for zero-order and twin-image elimination in digital off-axis holography, Appl. Opt. **39**, 4070 (2000).

[38] 10.5525/gla.researchdata.1224.